

# Dinitrogen Activation Upon Reduction of a Triiron(II) Complex\*\*

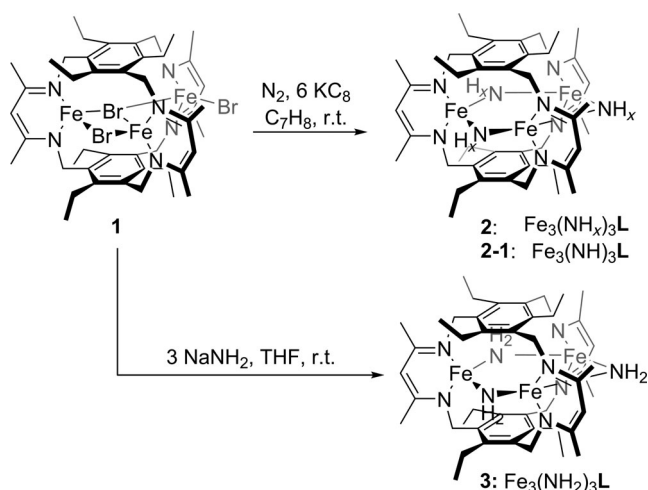
Yusoon Lee, Forrest T. Sloane, Geneviève Blondin, Khalil A. Abboud, Ricardo García-Serres,\* and Leslie J. Murray\*

**Abstract:** Reaction of a trinuclear iron(II) complex,  $\text{Fe}_3\text{Br}_3\text{L}$  (**1**), with  $\text{KC}_8$  under  $\text{N}_2$  leads to dinitrogen activation products (**2**) from which  $\text{Fe}_3(\text{NH})_3\text{L}$  (**2-1**; **L** is a cyclophane bridged by three  $\beta$ -diketiminate arms) was characterized by X-ray crystallography.  $^1\text{H}$  NMR spectra of the protonolysis product of **2** synthesized under  $^{14}\text{N}_2$  and  $^{15}\text{N}_2$  confirm atmospheric  $\text{N}_2$  reduction, and ammonia is detected by the indophenol assay (yield ~30%). IR and Mössbauer spectroscopy, and elemental analysis on **2** and **2-1** as well as the tri(amido)triiron(II) **3** and tri(methoxy)triiron **4** congeners support our assignment of the reduction product as containing protonated N-atom bridges.

In the Haber–Bosch process, dinitrogen is proposed to bind in a bridging fashion to iron atoms on the (111) face of the Mittasch catalyst.<sup>[1,2]</sup> Biological nitrogen fixation by nitrogenase occurs at the polynuclear iron face of the iron–molybdenum cofactor (FeMoco) after initial reductive elimination of  $\text{H}_2$ ,<sup>[3,4]</sup> however, whether  $\text{N}_2$  binds to one metal center or in a bridging mode to multiple ions remains uncertain.<sup>[5]</sup> Multimetallic assemblies of Ta,<sup>[6]</sup> Zr,<sup>[7]</sup> Mo,<sup>[8]</sup> and Fe<sup>[9]</sup> are either capable of or proposed to be involved in  $\text{N}_2$  activation in molecular systems. Across this breadth of examples, a theme of multiple metal ions reacting in a cooperative fashion appears central to activation of  $\text{N}_2$ . Surprisingly however, no synthetic polynuclear complexes have been reported that use a designed approach to interrogate the role, if any, or to control metal-ion cooperativity

for  $\text{N}_2$  reduction. To address this specific question, we have used ligands to template the assembly of trinuclear metal clusters.<sup>[10]</sup> Herein, we report the reduction of dinitrogen to terminally reduced N-atom ligands upon treatment of a tri-iron(II) complex with  $\text{KC}_8$  under an  $\text{N}_2$  atmosphere. To our knowledge, this system represents the first example of a designed multimetallic complex capable of cleaving the triple bond in dinitrogen.

Treatment of a red slurry of **1** with  $\text{KC}_8$  in toluene under  $\text{N}_2$  followed by filtration and pentane diffusion into a toluene solution of the crude filtrate afforded dark brown crystals, **2** (Scheme 1, ~40%). In scarce occasions, a minority product



**Scheme 1.** Synthesis of **2** and **3**.

cocrystallized with **2** as dark brown needles for which X-ray diffraction revealed a dimeric structure (Figure S11).  $^1\text{H}$  NMR spectra of the product of protonolysis of **2** synthesized under  $^{14}\text{N}_2$  and  $^{15}\text{N}_2$  (**2'**) confirm reduction of atmospheric  $\text{N}_2$  (Figure S1). Using the indophenol assay,<sup>[9a,11]</sup> we observed a relatively low yield of  $\text{NH}_3$  from **2** ( $30 \pm 2\%$ ) given the equivalents of  $\text{KC}_8$  per iron center used in the reaction. Our result here contrasts the higher yields reported for  $\text{N}_2$  reduction by an iron  $\beta$ -diketiminate and trigonal-pyramidal  $\text{P}_3\text{X}$  ( $\text{X} = \text{B}, \text{C}$ ) iron complexes.<sup>[9a,12]</sup> To probe whether incomplete dissociation of the  $\text{N}_2$ -derived ligands was responsible for the low  $\text{NH}_3$  yield, we assayed ammonia released from  $\text{Fe}_3(\text{NH}_2)_3\text{L}$  (**3**) synthesized by reaction of  $\text{NaNH}_2$  with **1**. Surprisingly, only 30% of the bridging amide ligands in **3** were detected as ammonia. Acids other than  $\text{HCl}$  failed to improve the  $\text{NH}_3$  yield from either **2** or **3**. No ammonia was observed for samples of **1** reduced under Ar, which agrees with activation of atmospheric  $\text{N}_2$  and not ligand

[\*] Y. Lee, F. T. Sloane, Prof. Dr. L. J. Murray  
Center for Catalysis, Department of Chemistry  
University of Florida  
Gainesville, FL 32611-7200 (USA)  
E-mail: murray@chem.ufl.edu

Dr. K. A. Abboud  
Department of Chemistry, University of Florida  
Gainesville, FL 32611-7200 (USA)

Dr. G. Blondin, Dr. R. García-Serres  
Université Grenoble Alpes, LCBM  
F-38054 Grenoble (France)

and  
CNRS, UMR 5249, LCBM  
F-38054 Grenoble (France)

and  
CEA, DSV, IRTSV, LCBM, pmb  
F-38054 Grenoble (France)  
E-mail: ricardo.garcia@cea.fr

[\*\*] L.J.M.: University of Florida and ACS Petroleum Research Fund (ACS-PRF 52704-DN13), an NSF departmental instrumentation award (CHE-1048604); HT. K.A.A.: NSF (CHE-0821346) and UF for funding X-ray equipment purchase. R.G.S.: Labex ARCAN (ANR-11-LABX-0003-01).

Supporting information for this article is available on the WWW under <http://dx.doi.org/10.1002/anie.201409676>.

decomposition. The indophenol assay was also conducted on crude reduction products of **1** by 3, 4, 5, 6, or 10 equiv  $\text{KC}_8$  in the presence of  $\text{N}_2$  (data not shown). Ammonia was detected in all cases with the highest yield recorded for the reaction with 6 equivalents.

We observed consistent morphologies and comparable unit cell parameters for crystals isolated from several different reduction reactions. We therefore selected one of the crystals from a sample of **2** and determined the molecular structure (**2-1**). Disorder is observed in the structure solution; however, the occupancies of the bridging N atoms N7–N9 and Fe1 are best modeled as 100 % and of Fe2 and Fe3 as 95 %. In this higher occupancy solution, the  $\text{Fe}_3\text{X}_3$  core in **2-1**, in which X denotes the donor atom in the bridging ligands, adopts a planar hexagonal arrangement with each iron center in a distorted tetrahedral geometry ( $\tau_4 = 0.92\text{--}0.94$ ; Figure 1).<sup>[13]</sup>

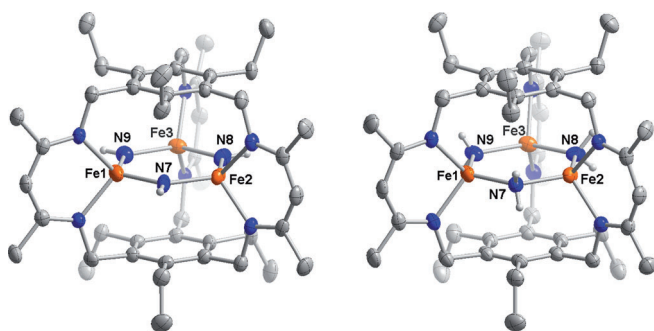


**Figure 1.** Solid-state structures of **2-1** (left) and **3** (right) at 65 % thermal ellipsoid. The pentane solvent molecule cocrystallized in **2-1** and hydrogen atoms have been omitted for clarity, except for the bridging nitrogen-bonded ones. C, H, N, and Fe atoms are depicted as gray, white, blue, and orange ellipsoids or spheres.

This structure type is unprecedented in iron cluster chemistry, but not unexpected given the steric constraints imposed by our ligand. Similar  $\text{Fe}_3\text{X}_3$  arrangements are observed in two other complexes, **3** and **4**, in which the N-atom of the  $\mu$ -amide and O-atom of the  $\mu$ -methoxide donors are coplanar with the three iron centers (Figures 1 and S2). In **2-1**, the H-atom bonded to each bridging N-atom ligand was readily located in the difference map and freely refined, implying a formulation of **2-1** as  $\text{Fe}^{\text{III}}_3(\text{NH})_3\text{L}$ . As anticipated with a higher oxidation state of the metal centers in **2-1** as compared to **3**, the Fe– $\mu\text{N}$  bonds (1.960(3)–1.978(3) Å) are shorter than observed for the Fe– $\text{NH}_2$  bonds in **3** (Table S2). Interestingly, the shortening of Fe– $\mu\text{N}$  bond results in slightly more acute diketiminate (nacnac) bite angles ( $\sim 95^\circ$ ) at each iron center (e.g., N1–Fe1–N2) in **2-1** relative to those in **3** ( $\sim 96^\circ$ ), shorter distances between the two N-atom donors of each nacnac arm (2.993(3)–3.009(3) Å for **2-1** versus 3.013(3)–3.034(3) Å for **3**), and compression of the cyclophane cavity in **2-1** relative to **3**. The bonds and angles around each iron center in **2-1** and **3** are significantly larger than those reported for mononuclear or self-assembled polynuclear iron  $\beta$ -diketiminate compounds.<sup>[9a,14]</sup> These correlated structural parameters all hint at the unique steric effects imposed by the macrobicyclic ligand, which arise from the limited range of allowable metal–

metal distances coupled to the size of the ancillary donor atoms. With respect to the disorder in the structure, we observe two iron centers, each coordinated  $\eta^6$  to the internal face of benzene caps of the ligand with low occupancies ( $\sim 5\%$ ; Figure S3). These iron centers could arise from a nacnac-to-arene shift, which is observed upon reduction of monometallic nacnac complexes, and suggests that low-valent iron centers are generated upon reduction of **1**.<sup>[15,16]</sup>

Consistent with  $\text{NH}_x$  donors in **2** and **2-1**, a weak IR absorption at  $3397\text{ cm}^{-1}$  is observed in spectra of **2** that shifts to  $3390\text{ cm}^{-1}$  for samples reduced under  $^{15}\text{N}_2$  (**2'**). This difference is in excellent agreement with a simple reduced-mass calculation for an NH bond, and the absorption is at comparable energy to other reported  $\mu$ -imide and  $\mu$ -amide donors.<sup>[17–19]</sup> These IR data and the observed H-atoms in the difference map provide strong evidence for protonated  $\text{N}_2$ -derived ligands in the isolated compound. Expectedly, an absorption feature at coincident energy is also present in IR spectra of  $\text{Fe}_3(\text{NH}_2)_3\text{L}$  (**3**) that has similar intensity relative to other ligand vibrations. We also observed a feature at  $3657\text{ cm}^{-1}$  in the IR spectrum of **2**, which is comparable to reported OH vibrations in related compounds.<sup>[20]</sup> This absorption is absent from the crude reaction product, is present only after crystallization, and is not observed in spectra of **3** and **4** (Figure S12). Significant incorporation of OH ligands in **2** is unlikely based on our elemental analysis data for which C, H, N, and Fe contents account for 99.87 % of the sample mass.

To gain further insight into the electronic structure and oxidation state of the iron sites, we studied **2** by Mössbauer spectroscopy. The zero-field Mössbauer spectra of **2** are composed of four quadrupole doublets, each of which accounts for ca. 25 % of total iron in the sample (Figure 2). The doublet formed by the two outermost absorptions is also detected in samples of  $\text{Fe}_3(\text{NH}_2)_3\text{L}$  (**3**) and  $\text{Fe}_3(\text{OMe})_3\text{L}$  (**4**), although the intensities of this doublet vary between the spectra (Figure S8). This common feature is assigned to an exogenous complex and subtracted from the spectra. This exogenous species likely arises from complex decomposition and is not present in spectra collected on the crude reaction filtrate (i.e., prior to crystallization, Figure S9). The three iron centers in **2-1** are crystallographically inequivalent, in agreement with the three distinct quadrupole doublets observed in spectra of **2**. Two of these doublets have parameters that are comparable to those determined for **3**, and the third doublet is consistent with an  $\text{Fe}^{\text{III}}$  center ( $\delta = 0.56\text{ mm s}^{-1}$ ,  $\Delta E_Q = 1.49\text{ mm s}^{-1}$  at 4.2 K). A careful examination of the temperature-dependence of each doublet's isomer shift in spectra of **2** (Table 1) indicates that the ferric site contains an admixture of  $\text{Fe}^{\text{II}}$  and vice versa (i.e., one of the  $\text{Fe}^{2+}$  sites contains admixture of  $\text{Fe}^{3+}$ ). This is only possible if the  $\text{Fe}^{2+}$  and  $\text{Fe}^{3+}$  sites are both present in the same complex. This feature is absent in spectra of the all-ferrous complex **3** (Figure S10). From our Mössbauer analysis, we conclude that **2** contains mainly mixed-valent triiron(II/II/III) complexes, although other combinations of oxidation states are likely present as minor products, their doublets largely overlapping with those of the former. The doublets observed in **2** are present in Mössbauer spectra of the crude reaction filtrate but in

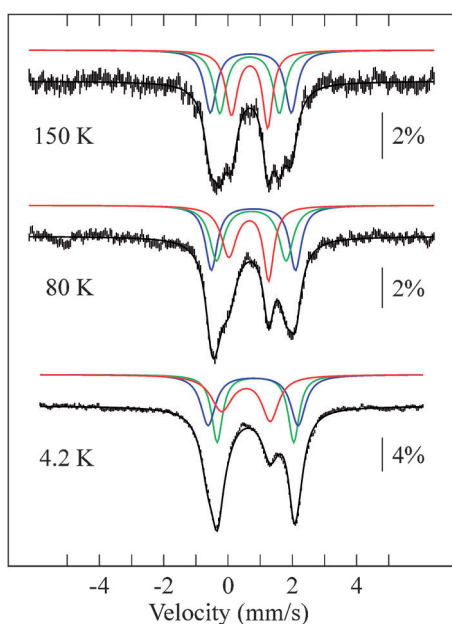


**Figure 2.** Variable-temperature Mössbauer spectra of **2** in zero field or in a 600 G applied magnetic field. A doublet (23 % of total iron) and assigned to an exogenous complex (Figure S8) is subtracted from each spectrum. The black solid lines overlaid with the experimental points are theoretical simulations. Spectra are simulated with three quadrupole doublets of equal integrations (see Table 1) represented by the colored lines: **2a** red, **2b** green, **2c** blue. Doublets **2b** and **2c** have parameters indicative of high-spin Fe<sup>II</sup>, whereas the isomer shift of **2a** is more consistent with a ferric site. This assignment is confirmed by the large linewidth and asymmetry of the red doublet, especially at lower temperatures, which are characteristic of half-integer spin systems. The respective temperature dependence of the isomer shifts of sites **2a** and **2b** (Table 1) suggests thermally assisted electron hopping between the two.<sup>[21]</sup>

**Table 1:** Simulation parameters for different quadrupole doublets in Mössbauer spectra of **2** measured at various temperatures.<sup>[22]</sup>

doublet	T [K]	$\delta$ [mm s <sup>-1</sup> ]	$\Delta E_Q$ [mm s <sup>-1</sup> ]	$\Gamma$ [mm s <sup>-1</sup> ]
<b>2a</b>	4.2	0.56	1.51	0.80/0.62
	80	0.65	1.24	0.57/0.39
	150	0.67	1.13	0.44/0.37
<b>2b</b>	4.2	0.85	2.38	0.41
	80	0.73	2.16	0.53
	150	0.67	1.85	0.45
<b>2c</b>	4.2	0.78	2.80	0.55
	80	0.79	2.61	0.44
	150	0.71	2.52	0.45

proportions consistent with a triiron(II/III/III) complex as the main product (Figure S9). Thus, **2** can be formulated as a cocrystallization of triiron complexes containing different mixtures of Fe<sup>2+</sup> and Fe<sup>3+</sup> ions. The overall packing is likely dominated by the ethyl substituents and the nearly C<sub>3</sub>-symmetric positions of the nacnac arms, which allows complexes with closely related structures to pack into unit cells with indistinguishable parameters. For example, unit cell

parameters for **2-1** are within error of those for **3**. The fact that the X-ray structure of **2-1** unambiguously assigns it as a formal triferric complex is hardly surprising, as the choice of a crystal for X-ray analysis is dictated by the quality of the diffraction pattern, and a symmetric complex is likely to yield less disorder in the lattice. In addition, the apparent evolution of species observed by Mössbauer suggests that time to analysis may influence product speciation. Answers to these questions will require further and detailed mechanistic studies, which is beyond the scope of this report. The central result however remains clear: data are all consistent with the cleavage of the N≡N bond upon reduction of our designed triiron(II) complex.

Two questions are apparent from the structure of **2-1** and the IR data indicating protonation of the N bridges in **2**. First, three N-atoms are present in each cluster. Two such donors would be consistent with intracomplex reduction of N<sub>2</sub> to afford an [Fe<sub>3</sub>N<sub>2</sub>] species; however, the third N-atom donor implies an intercluster cooperative process in which N<sub>2</sub> is cleaved across the interface between two clusters. Although the approach of two cyclophane complexes can seem sterically hindered, it does occur, as evidenced by the dimeric compound cocrystallized with **2** (Figure S11). This product is infrequently obtained and, when present, is a minor product based on crystal count under the microscope—the two crystal types are very different in aspect, color, and unit cell parameters. Although the structure of the dimer is highly disordered and complete characterization is lacking, the structure importantly demonstrates that two K<sup>+</sup> ions can bridge two triiron complexes to generate a dimeric species. Here, the preassembly of the triiron cluster using our ligand preserves the reactivity beyond the first equivalent of N<sub>2</sub> per three iron centers as compared to similar monometallic compounds. We attempted to isolate crystalline products from reduction reactions in which fewer reducing equivalents were used, but the major products for these reactions were consistent with either **1** or **2** based on crystallographic data and IR spectroscopy (Table S5, Figures S12–S16). This result highlights a difference in our designed multimetallic complex as compared to monometallic ones: reduction funnels the reaction toward complete cleavage of N<sub>2</sub> through likely both intra- and inter-complex cooperativity.<sup>[9a,23]</sup> Our attempts to first generate and isolate a reduced complex under Ar afforded a mixture of products in which one cluster contained partial occupancy of Fe atoms coordinated to the benzene caps within the internal cavity (data not shown). Given the complexity of these mixtures, we interrogated the reactivity of **1** with KC<sub>8</sub> under an N<sub>2</sub> atmosphere.

Second, each μ<sub>2</sub>-N donor in **2-1** is protonated, which suggests that intermediates either abstract H-atoms from other species in solution or react with adventitious proton sources (e.g., glass surface). Protonation of transient nitride or hydrazide complexes would be analogous to the reaction of low-valent mononuclear Fe–N<sub>2</sub> and Mo–N<sub>2</sub> complexes with Lewis acids,<sup>[12a,24]</sup> coordination of alkali cations to bridging nitride donors in iron clusters,<sup>[9a]</sup> and protonation of N<sub>2</sub> bound to reduced FeMoco.<sup>[5]</sup> X–H (X = C or O) bond activation is also known for mononuclear late 3d metal nitride and imide complexes and has been observed in N<sub>2</sub> activation by Zr



complexes.<sup>[7,8c,15,25–27]</sup> In an effort to limit access to protons and to isolate precursors to **2**, reactions were performed in silylated glassware but this treatment had no effect on the yield, crystallization, and identity of the complex based on X-ray crystallography and IR data (Table S5). Similarly, no changes were observed to the N–H vibrational mode for reactions performed in [D<sub>8</sub>]toluene, eliminating bulk solvent as the H<sup>+</sup> or H-atom source (Figure S17). Given the number of weak C–H bonds in the ligand, H<sup>+</sup> or H-atom abstraction from unreacted **1** by an N<sub>2</sub> reduction intermediate cannot be excluded. With this in mind, we also carried out the reduction of **1** in the presence of 9,10-dihydroanthracene (DHA) or [D<sub>4</sub>]DHA as a source of weak C–H/D bonds; however, we did not observe differences in the IR spectrum (Figure S18). This preliminary result suggests that H-atom abstraction from DHA does not occur, hinting at protonation rather than bond activation. We cannot rule out steric effects as the ethyl substituents could hinder the approach of DHA, and further investigations with smaller H-atom source will be required.

In conclusion, we report the first designed multinuclear complex capable of activating dinitrogen upon reduction. The reactivity is distinct from mononuclear analogues as the reaction funnels toward cleavage of three molecules of N<sub>2</sub> by two clusters even in the presence of a substoichiometric amount of KC<sub>8</sub>, and likely harnesses both intra- and intermolecular redox cooperativity.

Received: October 1, 2014

Revised: November 9, 2014

Published online: December 11, 2014

**Keywords:** cyclophanes · dinitrogen activation · iron clusters · macrobicycles · redox cooperativity

- [1] A. Hellman, E. J. Baerends, M. Biczysko, T. Bligaard, C. H. Christensen, D. C. Clary, S. Dahl, R. van Harrevelt, K. Honkala, H. Jonsson, G. J. Kroes, M. Luppi, U. Manthe, J. K. Nørskov, R. A. Olsen, J. Rossmeisl, E. Skúlason, C. S. Tautermann, A. J. C. Varandas, J. K. Vincent, *J. Phys. Chem. B* **2006**, *110*, 17719–17735.
- [2] a) H.-J. Freund, B. Bartos, R. P. Messmer, M. Grunze, H. Kühlenbeck, M. Neumann, *Surf. Sci.* **1987**, *185*, 187–202; b) M. Grunze, M. Golze, W. Hirschwald, H.-J. Freund, H. Pulm, U. Seip, M. C. Tsai, G. Ertl, J. Küppers, *Phys. Rev. Lett.* **1984**, *53*, 850–853.
- [3] P. C. Dos Santos, R. Y. Igarashi, H.-I. Lee, B. M. Hoffman, L. C. Seefeldt, D. R. Dean, *Acc. Chem. Res.* **2005**, *38*, 208–214.
- [4] a) R. Y. Igarashi, M. Laryukhin, P. C. Dos Santos, H.-I. Lee, D. R. Dean, L. C. Seefeldt, B. M. Hoffman, *J. Am. Chem. Soc.* **2005**, *127*, 6231–6241; b) B. M. Hoffman, D. Lukoyanov, D. R. Dean, L. C. Seefeldt, *Acc. Chem. Res.* **2013**, *46*, 587–595; c) Z.-Y. Yang, N. Khadka, D. Lukoyanov, B. M. Hoffman, D. R. Dean, L. C. Seefeldt, *Proc. Natl. Acad. Sci. USA* **2013**, *110*, 16327–16332.
- [5] B. M. Hoffman, D. Lukoyanov, Z.-Y. Yang, D. R. Dean, L. C. Seefeldt, *Chem. Rev.* **2014**, *114*, 4041–4062.
- [6] M. D. Fryzuk, S. A. Johnson, B. O. Patrick, A. Albinati, S. A. Mason, T. F. Koetzle, *J. Am. Chem. Soc.* **2001**, *123*, 3960–3973.
- [7] a) J. A. Pool, E. Lobkovsky, P. J. Chirik, *Nature* **2004**, *427*, 527–530; b) M. D. Fryzuk, J. B. Love, S. J. Rettig, V. G. Young, *Science* **1997**, *275*, 1445–1447.
- [8] a) C. E. Laplaza, C. C. Cummins, *Science* **1995**, *268*, 861–863; b) C. E. Laplaza, M. J. A. Johnson, J. C. Peters, A. L. Odom, E. Kim, C. C. Cummins, G. N. George, I. J. Pickering, *J. Am. Chem. Soc.* **1996**, *118*, 8623–8638; c) K. Arashiba, Y. Miyake, Y. Nishibayashi, *Nat. Chem.* **2011**, *3*, 120–125; d) T. Miyazaki, H. Tanaka, Y. Tanabe, M. Yuki, K. Nakajima, K. Yoshizawa, Y. Nishibayashi, *Angew. Chem. Int. Ed.* **2014**, *53*, 11488–11492.
- [9] a) M. M. Rodriguez, E. Bill, W. W. Brennessel, P. L. Holland, *Science* **2011**, *334*, 780–783; b) T. M. Figg, P. L. Holland, T. R. Cundari, *Inorg. Chem.* **2012**, *51*, 7546–7550.
- [10] a) G. L. Guillet, F. T. Sloane, M. F. Dumont, K. A. Abboud, L. J. Murray, *Dalton Trans.* **2012**, *41*, 7866–7869; b) G. L. Guillet, F. T. Sloane, D. M. Ermert, M. W. Calkins, M. K. Peprah, E. S. Knowles, E. Čizmar, K. A. Abboud, M. W. Meisel, L. J. Murray, *Chem. Commun.* **2013**, *49*, 6635–6637; c) G. N. Di Francesco, A. Gaillard, I. Ghiviriga, K. A. Abboud, L. J. Murray, *Inorg. Chem.* **2014**, *53*, 4647–4654; d) L. J. Murray, W. W. Weare, J. Shearer, A. D. Mitchell, K. A. Abboud, *J. Am. Chem. Soc.* **2014**, *136*, 13502–13505.
- [11] A. L. Chaney, E. P. Marbach, *Clin. Chem.* **1962**, *8*, 130–132.
- [12] a) J. S. Anderson, J. Rittle, J. C. Peters, *Nature* **2013**, *501*, 84–87; b) S. E. Creutz, J. C. Peters, *J. Am. Chem. Soc.* **2014**, *136*, 1105–1115.
- [13] L. Yang, D. R. Powell, R. P. Houser, *Dalton Trans.* **2007**, 955–964.
- [14] J. M. Smith, R. J. Lachicotte, P. L. Holland, *Chem. Commun.* **2001**, 1542–1543.
- [15] R. E. Cowley, P. L. Holland, *Inorg. Chem.* **2012**, *51*, 8352–8361.
- [16] T. R. Dugan, X. Sun, E. V. Rybak-Akimova, O. Olatunji-Ojo, T. R. Cundari, P. L. Holland, *J. Am. Chem. Soc.* **2011**, *133*, 12418–12421.
- [17] S. D. Brown, M. P. Mehn, J. C. Peters, *J. Am. Chem. Soc.* **2005**, *127*, 13146–13147.
- [18] M. García-Castro, A. Martín, M. Mena, J.-M. Poblet, C. Yélamos, *Eur. J. Inorg. Chem.* **2006**, 1155–1160.
- [19] C. Ni, H. Lei, P. P. Power, *Organometallics* **2010**, *29*, 1988–1991.
- [20] a) Y. Yu, A. R. Sadique, J. M. Smith, T. R. Dugan, R. E. Cowley, W. W. Brennessel, C. J. Flaschenriem, E. Bill, T. R. Cundari, P. L. Holland, *J. Am. Chem. Soc.* **2008**, *130*, 6624–6638; b) M. D. Walter, P. S. White, *Dalton Trans.* **2012**, *41*, 8506–8508.
- [21] A. S. Borovik, M. P. Hendrich, T. R. Holman, E. Münck, V. Papaefthymiou, L. Que, Jr., *J. Am. Chem. Soc.* **1990**, *112*, 6031–6038.
- [22] The three doublets were simulated with equal integrations. Compound **2a** is assigned to a ferric center, whereas **2b** and **2c** are characteristic of tetrahedral coordinated ferrous centers. The quadrupole splittings are strongly temperature-dependent, indicating the presence of low-lying excited states resulting from spin coupling between the iron centers. The isomer shift of **2c** decreases with increasing temperature as expected from a 2nd order Doppler shift (SOD). However, the isomer shift of **2b** has a much stronger decrease than what expected from SOD, and the isomer shift of **2a** increases with temperature. This suggests an admixture of ferric character from **2a** into the ferrous center **2b** and vice versa, the admixture increasing with temperature. Altogether, these results agree with an Fe<sup>III</sup>Fe<sup>II</sup>Fe<sup>II</sup> mixed-valent complex in which the valences are localized but experience thermally assisted electron hopping.<sup>[21]</sup>
- [23] a) K. Ding, A. W. Pierpont, W. W. Brennessel, G. Lukat-Rodgers, K. R. Rodgers, T. R. Cundari, E. Bill, P. L. Holland, *J. Am. Chem. Soc.* **2009**, *131*, 9471–9472; b) J. M. Smith, R. J. Lachicotte, K. A. Pittard, T. R. Cundari, G. Lukat-Rodgers, K. R. Rodgers, P. L. Holland, *J. Am. Chem. Soc.* **2001**, *123*, 9222–9223; c) J. M. Smith, A. R. Sadique, T. R. Cundari, K. R. Rodgers, G. Lukat-Rodgers, R. J. Lachicotte, C. J. Flaschenriem, J. Vela, P. L. Holland, *J. Am. Chem. Soc.* **2006**, *128*, 756–769;

- d) M. D. Fryzuk, T. S. Haddad, S. J. Rettig, *J. Am. Chem. Soc.* **1990**, *112*, 8185–8186.
- [24] D. V. Yandulov, R. R. Schrock, *Science* **2003**, *301*, 76–78.
- [25] J. J. Scepaniak, J. A. Young, R. P. Bontchev, J. M. Smith, *Angew. Chem. Int. Ed.* **2009**, *48*, 3158–3160; *Angew. Chem.* **2009**, *121*, 3204–3206.
- [26] R. E. Cowley, N. A. Eckert, S. Vaddadi, T. M. Figg, T. R. Cundari, P. L. Holland, *J. Am. Chem. Soc.* **2011**, *133*, 9796–9811.
- [27] E. A. MacLachlan, F. M. Hess, B. O. Patrick, M. D. Fryzuk, *J. Am. Chem. Soc.* **2007**, *129*, 10895–10905.
-